GeoAmericas2020
4th PAN AMERICAN CONFERENCE ON GEOSYNTHETICS
26-29 APRIL 2020 • RIO DE JANEIRO • BRAZIL

Modeling geogrid-reinforced foundation considering particle and geogrid shapes

Ge Gao, Graduate Student, Civil Engineering and Applied Mechanics, McGill University, Canada
Email: ge.gao2@mail.mcgill.ca
Mohamed Meguid, Professor, Civil Engineering and Applied Mechanics, McGill University, Canada
Email: mohamed.meguid@mcgill.ca
Luc Chouinard, Associate Professor, Civil Engineering and Applied Mechanics, McGill University, Canada
Email: luc.chouinard@mcgill.ca

ABSTRACT
Geogrid reinforcement has been extensively used over the past few decades to enhance the stability and load carrying capacity of different geomaterials. Understanding soil-geogrid interaction is essential for the analysis and design of geogrid-reinforced structures. A three-dimensional discrete element model that is capable of capturing the response of granular material with geogrid inclusion is developed in this study. The 3D shape of the crushed limestone is modelled by tracing the surface area of a typical particle and fitting a number of bonded spheres into the generated surface. Model calibration is performed using triaxial and direct shear tests to determine the microparameters that allow for the stress-strain behavior of the backfill material to be replicated. The model is validated using experimental data and applied to simulate a series of crushed limestone reinforced with geogrid and subjected to surface loading. The analysis allows for the explicit geometry of the geogrid and the discontinuous nature of the soil to be captured. This study suggests that modeling the 3D geogrid geometry is important to accurately capture the geogrid response under both confined and unconfined conditions. Accounting for the particle shape in the analysis can significantly enhance the predicted response of the geogrid-soil system. The calculated response confirms the observed behaviour of reinforced sands and explains the increase in load carrying capacity of reinforced systems used in different geotechnical engineering applications. The proposed modelling approach has proven to be efficient in modelling this class of problems and can be adapted for other reinforced soil applications.

Keywords: Geogrid; Geogrid-reinforced foundation; Numerical analysis; Particle shape; Discrete element method

1. INTRODUCTION

Geogrid has been successfully used for the reinforcement of different geotechnical structures (e.g. railway tracks, road embankments, foundations and retaining walls). Their three-dimensional open structure, which interlocks with the surrounding soil, creates a cost effective earth structure (Koerner, 1994).
Finding the interaction mechanism between soil and geogrid is important in the design and analysis of geogrid-reinforced structures. Extensive research still has been conducted to investigate the interaction mechanism between geogrid and the surrounding soil using experimental and theoretical studies (Shin and Das, 2010; Indraratna et al. 2011; Miyata and Bathurst 2012; Lin et al., 2013; Ezzein and Bathurst, 2014; Bathurst and Ezzein, 2015; Mosallanezhad et al. 2016; Han et al. 2018; Xu et al. 2019). Transparent soil has been used by Bathurst and Ezzein (2017) to allow for the movement of the reinforcement layer to be monitored. The finite element (FE) method has been used by researchers to model soil-geogrid interaction (Rowe and Liu, 2015; Hussein and Meguid, 2016; Zhuang and Wang, 2016; Hussein and Meguid, 2019). One inherent limitation of continuum methods is the difficulty in analyzing soil-geogrid interaction at the particle level (Gao and Meguid 2018c).
The discrete element method (DEM) (Cundall and Strack, 1979), has a particular advantage in capturing the kinematic behaviours and microscopic responses of discontinuous media (Stahl and Konietzky, 2011; Gao and Meguid, 2018a&b; Lai and Chen, 2017; Zhang and Evans 2018; Shen et al., 2019; Sun et al. 2019; Sun and Zheng 2019; Zhang and Evans 2019). The method has also been successfully used to investigate the interface behaviour of geogrid-soil system considering the discontinuous nature of granular particles. Lai et al. (2014) investigated geogrid-reinforced pile-supported embankment using DEM and found that the presence of geogrid is able to evidently improve the efficacy of load transfer and enhance the stability of soil arching. Miao et al. (2017) studied the effect of particle shape on the response of geogrid-reinforced systems under pullout loading and evaluated the effect of particle angularity on the interlocking behaviour of geogrid-reinforced ballast. The above studies demonstrated that the stress-strain behaviour of a geogrid material

embedded in backfill soil is complex, particularly for angular soil particles of irregular shapes as they interact with one or more geogrid layers (Gao and Meguid 2018c).
The objective of this study is to propose a 3D particulate model that is able to capture the response of both unconfined and soil confined biaxial geogrid embedded in irregular shaped material and subjected to surface loading. This is achieved in three phases as follows:
i) Modeling crushed limestone: The shape of a typical particle is simulated based on the type of material used in laboratory experiments. The input parameters needed for the discrete element analysis are determined using triaxial and direct shear tests.
ii) Developing particle-based geogrid model: A 3D geogrid model is created using parallel bonding between spheres. The model is validated using index test results to ensure that the response of the geogrid material is properly captured under tensile loading.
iii) Analyzing a case study: Using the created backfill and geogrid models, a case study involving a square footing over geogrid-reinforced soil is analyzed and the results are compared with experimental data.

2. IRREGULAR-SHAPED PARTICLES

In most DEM applications, granular materials are simplified as an assembly of round particles (disks in two dimensions and spheres in three dimensions) to keep the computational cost affordable; however, these simple shapes fail to reproduce the geometry-dependent material behavior, including particle interlocking and rolling resistance (Ma et al. 2014; Zhou et al. 2018). Researchers (e.g. Stahl and Konietzky, 2011; Chen et al., 2012; Stahl et al., 2014; Indraratna et al., 2014; Miao et al., 2017) have used clump logic in modeling complex-shaped particles in various applications. A clump is defined as a single rigid body of overlapping spherical pebbles of different sizes that acts as a single particle of a chosen or arbitrary shape (Gao and Meguid, 2018a&b). In this study, an approach has been developed to create irregular shaped particles based on the construction of a triangular mesh that traces the actual geometry of a typical crushed limestone particle (Fig. 1).

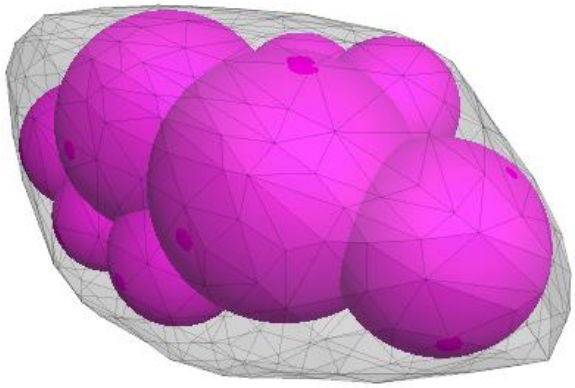

Fig. 1. Modeling crushed limestone particle.

3. MICRO-PARAMETER CALIBRATION

3.1 Triaxial compression test

Although several studies used discrete element analysis to study soil-geogrid interaction (e.g. Wang et al., 2016; Miao et al., 2017; Ngo et al., 2017; Lai et al., 2017), only a limited number of these studies fully calibrated the set of micro-parameters that govern the interface and interlocking effects, including the effective modulus, stiffness ratio (normal to shear stiffness ratio), peak and residual friction coefficients.
In this study, large-scale triaxial tests are used to determine the effective modulus of the contact that is needed for the discrete element analysis. A cylindrical sample 200 mm in diameter and 500 mm in height is modeled as shown in Fig. 2. A servo-mechanism is simulated and used to apply the confining pressures acting on samples in both axial and radial directions. Stahl and Konietzky (2011) demonstrated that modeling the loading-unloading phase of the triaxial tests allows for the deformability of the system to be determined with a reasonable accuracy. Therefore, the response of the particles under loading-unloading condition is simulated in this study at an average confinement pressure of 50 kPa and axial strain of up to 0.05% as illustrated in Fig. 2. The effective contact modulus and stiffness ratio are determined such that the elastic modulus matches that measured in the physical experiments (about 120 MPa).

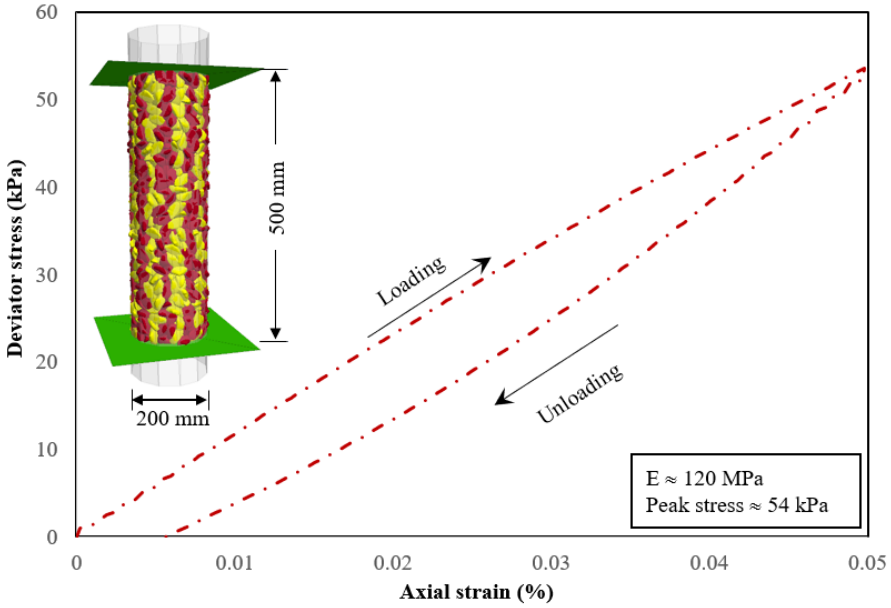

Fig. 2. Simulation of the triaxial compression test (confining pressure = 50 kPa).

3.2 Direct shear test

The direct shear tests were performed using a laboratory shear box measuring 304.8 mm × 304.8 mm × 130.9 mm under three different normal stresses, namely 25, 50 and 75 kPa. The measured friction angle was found to be 53° (Chen et al., 2009). The direct shear tests were numerically modeled considering the dimensions and boundary conditions used in the experiments. Four vertical boundaries (walls) and one horizontal boundary were used to represent the upper and lower parts of the box as shown in the insert plot of Fig. 3. An assembly of irregular shaped clumps is generated within the box and then the system is cycled to equilibrium. Normal stress is applied at the top of the sample and is kept constant using a servo-mechanism (Itasca, 2014). The lower part of the box is then moved horizontally at a velocity of 0.1 mm/s, which is consistent with that used in the experiments.

The calculated peak stresses are 36 kPa, 67 kPa and 102 kPa for applied normal stresses of 25, 50, and 75 kPa, respectively. These results are consistent with the measured values in the direct shear tests (Chen et al., 2009). Fig. 3 presents the relationship between normal and shear stresses for both peak and residual values. Results indicated that the peak and residual friction angles of the modeled particles are approximately 53° and 36°, respectively. Based on this analysis, the particle friction coefficient that produces these friction angles is found to be 0.32.

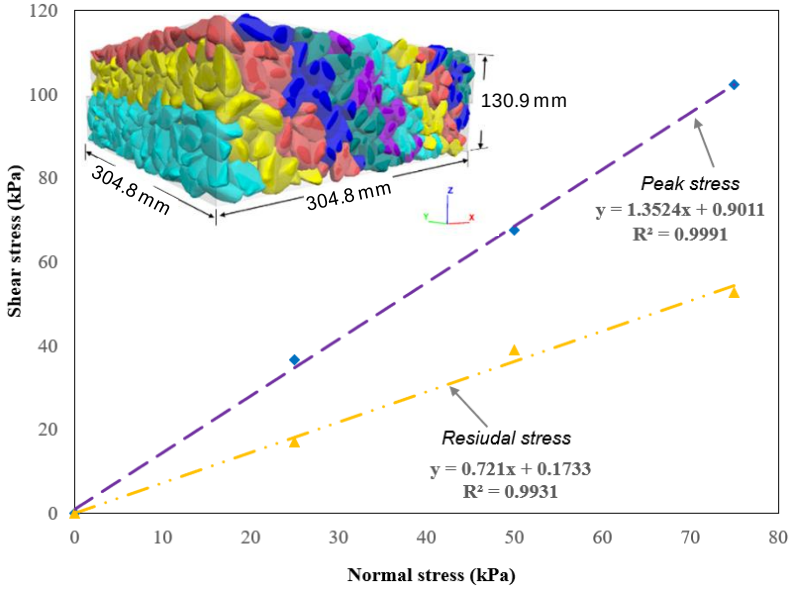

Fig. 3. Peak and residual shear stresses obtained using direct shear test.

To quantitatively assess the anisotropy features of the modeled material during shear, Fig. 4 shows the contact force network among the distinct particles at shear displacements of 0 mm, 4.93 mm, and 40.9 mm, respectively under normal stress of 75 kPa. Forces in a granular assembly are transferred through an interconnected network of force chains through contact points. Taking advantage of a DEM simulation, the contact force chains of irregular-shaped particle assembly were captured. The centers of the contacting particles are connected using lines with thicknesses that represent the magnitude of the contact forces (normal contact forces and tangential contact forces). In addition, the spatial contact normal distributions can be visualized with three-dimensional histograms in the region to better understand the development of force chains within the specimen. The shear strength of granular materials is generally attributed to the buildup of an anisotropic structure induced by shearing (Azéma et al., 2012). At the initial equilibrium (shear displacement = 0), the contact forces have identical distributions throughout the assembly and transmitted vertically from the top to the bottom of the direct shear box, corresponding to a desired isotropic stress state due to an isotropic compression. As shearing proceeds, the spherical histogram becomes elongated in the loading direction, which means that strong contact forces intensified in the loading direction, as shown in Fig. 4.

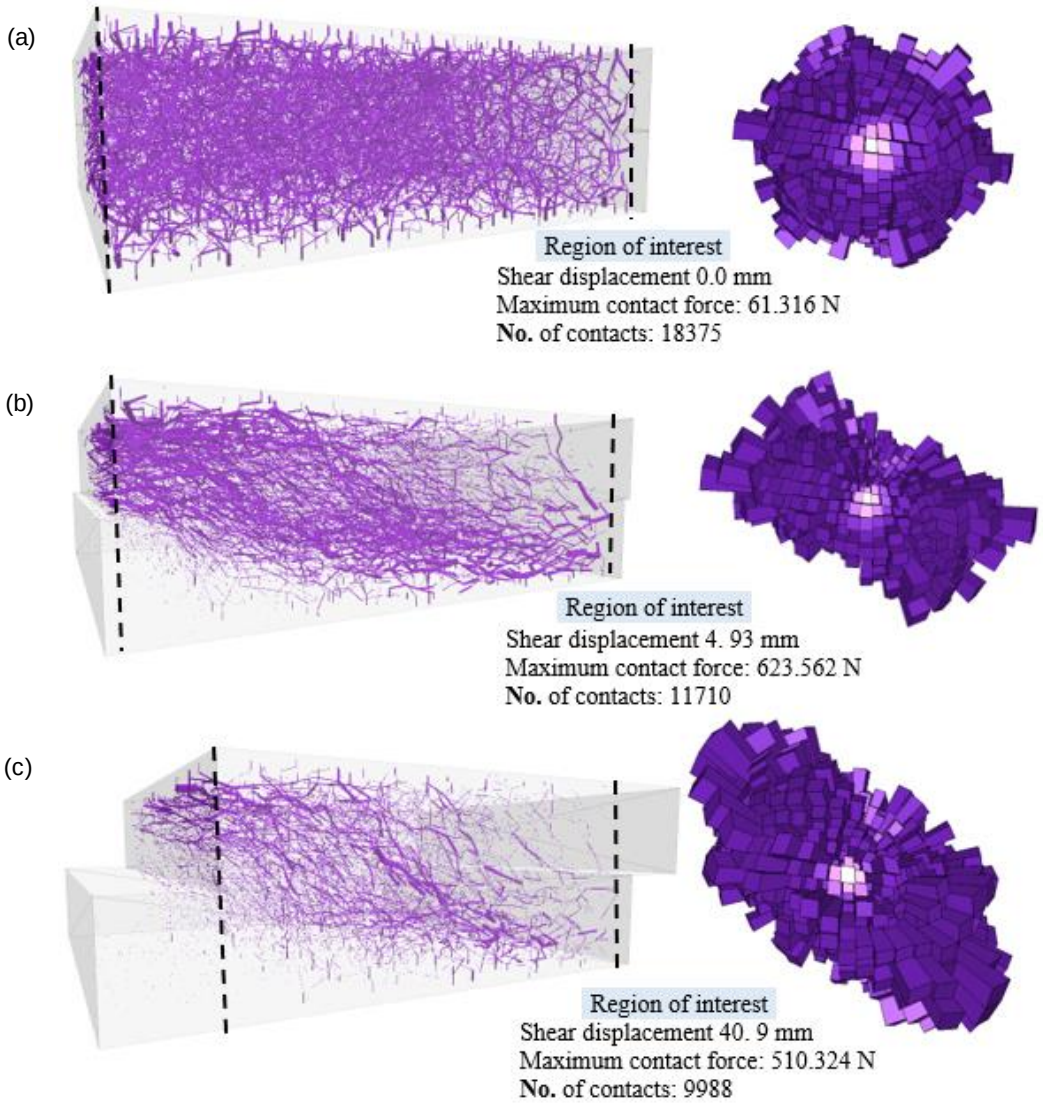

Fig. 4. Spatial distribution of contact forces and 3D histograms of contact normal at (a) initial state; (b) peak state and (c) residual state.

4. GEOGRID

The geogrid used in this study is modeled as strings of overlapping spherical particles joined by linear parallel bonds. Linear parallel bond allows for the geometrical and mechanical properties of the biaxial geogrid material to be properly

simulated (Miao et al. 2017; Gao and Meguid 2018c). The geogrid model consists of three main elements: longitudinal ribs, transverse bars and connecting junctions. Each longitudinal rib and transverse bar consists of 20 and 16 overlapping spherical particles, respectively. The diameter of these particles is 4 mm, which results in a uniform thickness for both the transverse and longitudinal members. In addition, each junction consists of eight particles arranged as shown in Fig. 5 to simulate junction rigidity. A series of tensile tests is performed to measure the load-displacement response of the biaxial geogrid samples (Hussein and Meguid, 2016). The tests were conducted according to the ASTM standard D6637-11 (2011) on multi-rib geogrid specimens in both the machine (MD) and the cross machine (XMD) directions, as depicted in Fig. 5.

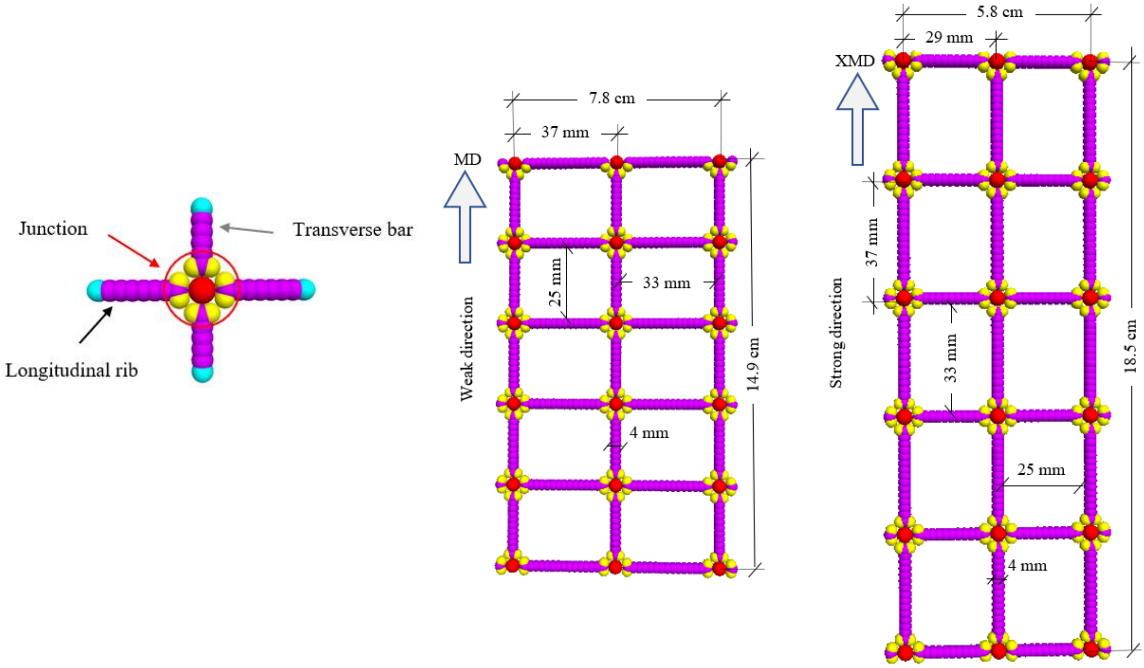

Fig. 5. Discrete element modeling of the multi-rib tensile test.

Uniaxial tensile tests are numerically simulated using the created geogrid model following the procedure and loading rate used in the experiments (10% strain/min). The microparameters, including the effective contact modulus, E, stiffness ratio, k_n/k_s, friction coefficient, μ, bond strength, bond effective modulus, $\overline{E}$ are adjusted such that the calculated response satisfies to a large extent that measured in the experiment (see Fig. 6). The calibrated geogrid mirco-parameters are summarized in Table 1.

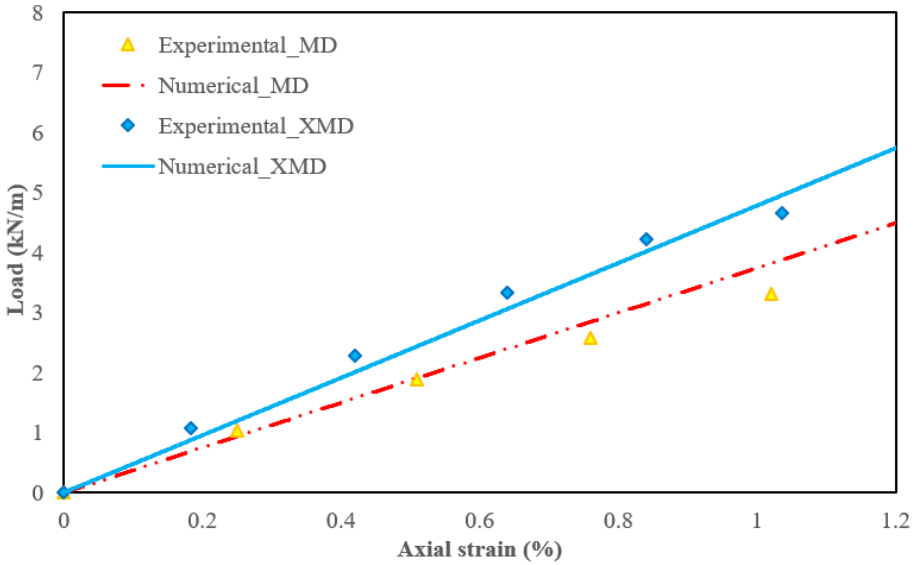

Fig. 6. Model performance: calculated versus measured responses of the geogrid in both the MD and XMD.

Table 1. Micromechanical parameters used for the geogrid model

Parameter	Assigned value
Particle density (Polypropylene)	900
Effective contact modulus (MPa)	0.1
Normal-to-shear stiffness ratio (*kn / ks)*	1.5
Bond effective modulus (MPa)	900
Bond normal-to-shear Stiffness ratio ($\overline{kn} / \overline{ks}$)	10^4
Parallel bond tensile strength (MPa)	100
Parallel bond cohesion (MPa)	100
Parallel bond friction angle (Degree)	0
Parallel radius multiplier (-)	1.0

5. GEOGRID-REINFORCED SYSTEM

The developed geogrid and particle models are used in this section to simulate the behavior of a reinforced soil system. To achieve this objective, the experimental results reported by Chen et al. (2009) are adopted. The setup consists of a rigid box 1.5 m in length, 0.91 m in width and 0.91 m in height that hosts the crushed limestone backfill material. Footing pressure was applied using a steel plate that measures 152 mm × 152 mm. Considering the twofold symmetry of the problem domain, only one-quarter of the geometry is modelled with symmetric boundary conditions as illustrated in Fig. 7. The granular assembly is generated layer by layer. One layer of particles is randomly distributed within a given area, and cycled sufficiently to gain a uniform distribution. Subsequently, the particles are compressed by moving down the top platen until the porosity of the first layer reaches the target value. The process is repeated for the overlying layers until the backfill height reaches the level of the geogrid layer. Two walls were generated below and above the geogrid sheet that is generated in the separate space enclosed by the pair of isolated walls, as shown in Fig. 7a. Additional details can be found in Jiang et al. (2003). During this process, the geogrid is kept motionless by fixing its velocity, and the gravity g and interparticle friction coefficient μ are set to zero. The interparticle friction μ is then turned on and the system is cycled to equilibrium. In addition, the pair of isolation walls is deleted to allow the geogrid to come in contact with the stone particles as shown in Fig. 7b. The rigid footing is simulated using a small wall 76 mm × 76 mm placed at the top of the compacted backfill and the load is applied incrementally to allow for the response of the system to be recorded for both the unreinforced and reinforced cases. It is worthwhile noting that the loading rate is slow enough to insure a quasi-static response.

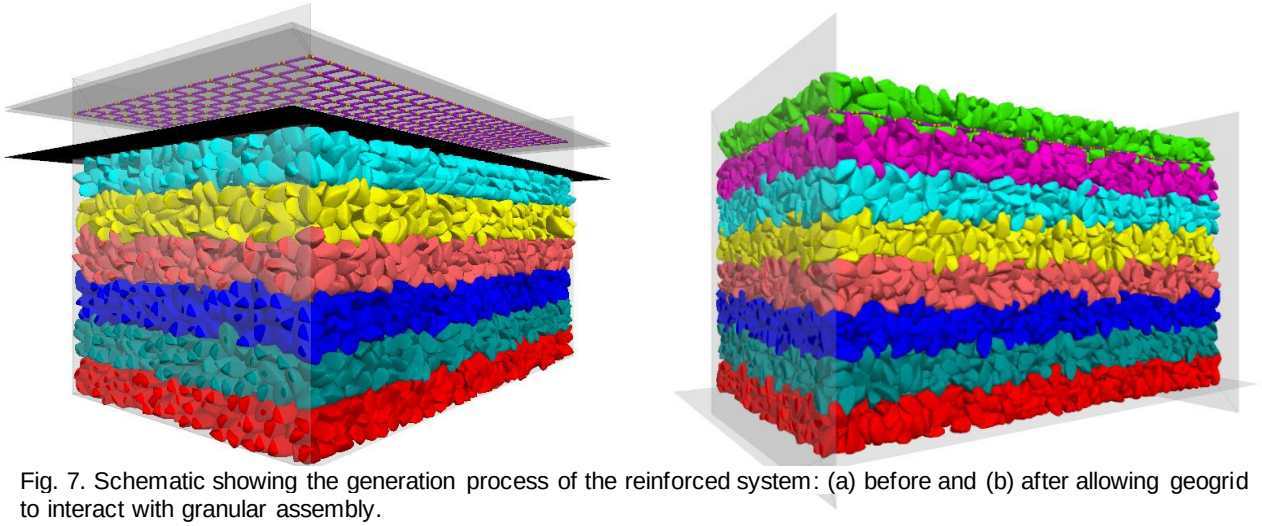

Fig. 7. Schematic showing the generation process of the reinforced system: (a) before and (b) after allowing geogrid to interact with granular assembly.

Fig. 8 shows the relationship between the equivalent footing pressure (calculated numerically) and the vertical settlement for the four investigated cases: unreinforced (N = 0) and reinforced using one (N = 1), two (N = 2) and three geogrid layers (N = 3). For the unreinforced case, excessive settlement started to develop at applied footing pressure of about 5 MPa as shown in Fig. 8. The irregular shaped clumps were found to replicate the correct stiffness and vertical displacement of the

footing up to applied pressure of about 5 MPa. Similar behaviour is found for the three reinforced cases where the model built using irregular shaped particles was able to capture the correct response of the geogrid-reinforced system for the entire loading range. It is worth noting that for both the unreinforced and reinforced cases, the models slightly underestimated the settlement of the footing as failure is approached. This can be explained by the fact that the used particle models do not allow for the additional settlement resulting from the possible particle crushing to be captured under high loading. It influences not only the physical state of the assembly (grain structure and porosity), but also the particle interaction (interparticle friction, contact force and coordination number).

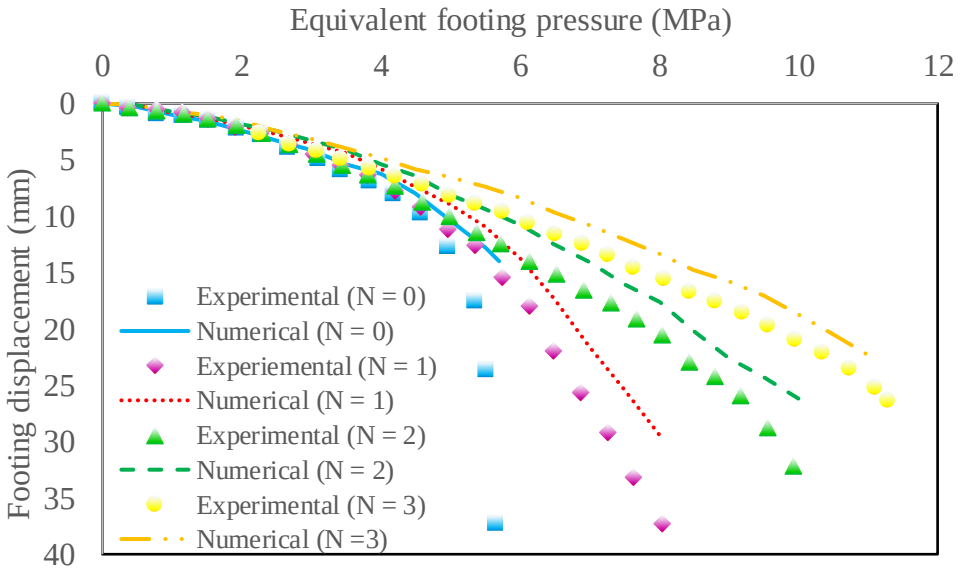

Fig. 8. Load-displacement relationships for: unreinforced N = 0; reinforced: N = 1; N = 2; N = 3.

SUMMARY AND CONCLUSIONS

A discrete element procedure for the 3D analysis of unconfined and soil-confined geogrid is developed in this study. The effect of particle shape on the response of geogrid embedded in crushed limestone material is simulated. The crushed limestone particles are modeled using irregular-shaped clumps. The governing microparameters (effective modulus, stiffness ratio, peak and residual friction coefficients) are first calibrated using a series of triaxial-compression and direct shear tests. A numerical model that is capable of simulating the response of the unconfined biaxial geogrid under tensile loading is then developed and validated using index test results. In developing this model, the details of the geometrical features are explicitly simulated. A procedure is also developed to simulate a reinforced soil system using the created clump particles and the geogrid sheet. A suitable particle packing using the undercompaction method is then adopted to allow for the interlocking effect to be properly captured without disturbing the initial position and orientation of the particles. To confirm the validity of the model, the calculated response is compared with existing experimental data for reinforced granular material with one or more geogrid layers under footing pressure. The introduction of clumped particles for modeling the irregular-shaped stones is found to form a mechanically stabilised layer, where particles interlock within the geogrid and become confined within the apertures creating an enhanced performance with respect to shear strength and dilation properties of the granular material. In addition, increasing the number of geogrid layers resulted in a significant increase in the ultimate bearing capacity of the reinforced soil system. Although the proposed discrete element approach does not consider particles breakage, the investigation on reinforced material has been shown to hold much promise in reliably capturing the correct response of a reinforced soil system.

REFERENCES

ASTM, 1997. Standard test method for nonrepetitive static plate load tests of soils and flexible pavement components, for use in evaluation and design of airport and highway pavements. pp. 112–113.

ASTM. (2015). “Standard test method for determining tensile properties of geogrids by the single or multi-rib tensile method.” D6637/D6637M–15, West Conshohocken, PA.

Bathurst, R.J., Ezzein, F.M. (2015). Geogrid and soil displacement observations during pullout using a transparent granular soil. Geotech. Test. J. 38 (5), 673-685.

Bathurst, R.J. and Ezzein, F.M. (2017). Insights into geogrid-soil interaction using a transparent granular soil. Géotechnique Letters 7: 1-5.

Chen, C., McDowell, G., Thom, N.H. (2012). Discrete element modelling of cyclic loads of geogrid-reinforced ballast under confined and unconfined conditions. Geotextiles and Geomembranes 35, 76-86.

Chen, Q., Abu-Farsakh, M., Sharma, R. (2009). Experimental and analytical studies of reinforced crushed limestone. Geotextiles and Geomembranes 27(5), 357–367.

Ezzein, F.M., Bathurst, R.J. (2014). A new approach to evaluate soil-geosynthetic interaction using a novel pullout test apparatus and transparent granular soil. Geotext. Geomembranes 42(3), 246-255.

Gao, G. and Meguid, M.A. (2018a). On the role of sphericity of falling rock clusters- Insights from experimental and numerical investigations. Landslides 15(2), 219-232.

Gao, G. and Meguid, M.A. (2018b). Modeling the impact of a falling rock cluster on rigid structures. ASCE International Journal of Geomechanics 18(2), 1-15.

Gao, G. and Meguid, M.A. (2018c). Effect of particle shape on the response of geogrid-reinforced systems: Insights from 3D discrete element analysis. Geotextiles and Geomembranes, 46(6), 685-698.

Jiang, M.J., Konrad, J.M., Leroueil, S., 2003. An efficient technique for generating homogeneous specimens for DEM studies. Computer and Geotechnics 30(7). 579-597.

Hussein, M.G. Meguid, M.A. (2016). A three-dimensional finite element approach for modeling biaxial geogrid with application to geogrid-reinforced soils. Geotextiles and Geomembranes 44(3), 295-307.

Hussein, M.G. Meguid, M.A. (2019). Improved understanding of geogrid response to pullout loading: Insights from three-dimensional finite element analysis. Canadian Geotechnical Journal, DOI: 10.1139/cgj-2018-0384.

Indraratna, B., Ngo, N.T. and Rujikiatkamjorn, C. (2011). Behavior of geogrid-reinforced ballast under various levels of fouling, Geotextile Geomembr., 29(3): 313–322.

Itasca. 2014., Particle flow code in three dimensions (PFC3D), Minneapolis.

Koerner, R.M. (1994). Designing with geosynthetics, 3rd ed. Prentice Hall, Englewood Cliff, NJ, USA.

Lai, Z., Chen, Q., 2017. Characterization and discrete element simulation of grading and shape-dependent behavior of JSC-1A Martian regolith simulant. Granular Matter 19(4), 69.

Lai, H.J., Zheng, J.J., Zhang, J., Zhang, R.J., Cui, L. (2014). DEM analysis of "soil"-arching within geogrid-reinforced and unreinforced pile-supported embankments. Computer and Geotechnics 61, 13-23.

Lin, Y.L., Zhang, M.X., Javadi, A.A., Lu, Y. and Zhang, S.L. (2013). Experimental and DEM simulation of sandy soil reinforced with H–V inclusions in plane strain tests. Geosynthetics International 20(3), 162-173.

Ma, G., Zhou, W., Chang, X.L., Yuan, W. (2014). Combined FEM/DEM modeling of triaxial compression tests for rockfills with polyhedral particles, Int. J. Geomechics., 14(4): 04014014.

Miao, C., Zheng, J., Zhang, R., Cui, L. (2017). DEM modeling of pullout behavior of geogrid reinforced ballast: The effect of particle shape. Computer and Geotechnics 81, 249-261.

Miyata, Y., Bathurst, R.J. (2012). Reliability analysis of soil-geogrid pullout models in Japan, Soils Found., 52(4): 620-633.

Mosallanezhad, M., Alfaro, M.C., Hataf, N., Sadat Taghavi, S.H. (2016). Performance of the new reinforcement system in the increase of shear strength of typical geogrid interface with soil, Geotext. Geomembr., 44: 457-462.

Ngo, N.T., Indraratna, B., Rujikiatkamjorn, C. (2017). A study of the geogrid–subballast interface via experimental evaluation and discrete element modelling. Granular Matter, 19(3): 54.

Rowe, R.K., Liu, K.W. (2015). Three-dimensional finite element modelling of a full-scale geosynthetic-reinforced, pile-supported embankment. Canadian Geotechnical Journal 52(12), 2041-2054.

Shen, W.G, Zhao, T., Dai, F., Jiang, M., Zhou, G.G.D. (2019). DEM analyses of rock block shape effect on the response of rockfall impact against a soil buffering layer. Eng. Geol., 249: 60-70.

Shin, E.C., Das, B.M. (2000). Experimental Study of Bearing Capacity of a Strip Foundation on Geogrid- Reinforced Sand. Geosynthetic International 7(1), 59-7.

Stahl, M., Konietzky, H., 2011. Discrete element simulation of ballast and gravel under special consideration of grain-shape, grain-size and relative density. Granular Matter 13 (4), 417-428.

Stahl, M., Konietzky, H., Kamp, L., Jas, H. (2014). Discrete element simulation of geogrid-stabilised soil. Acta Geotechnica 9(6), 1073-1084.

Sun, Q., Zheng, J., He, H., Li, Z. (2019). Particulate material fabric characterization from volumetric images by computational geometry. Powder Technol., 344: 804-813.

Sun, Q., Zheng, J. (2019). Two-dimensional and three-dimensional inherent fabric in cross-anisotropic granular soils, Comput. Geotech., 116: 103197.

Zhou, B., Wang, J., Wang, H.B. (2018). Three-dimensional sphericity, roundness and fractal dimension of sand particles. Géotechnique 68(1): 18-30.

Zhang, N., Evans, T. M. (2018). Three dimensional discrete element method simulations of interface shear. Soils and Foundations.

Zhang, N., Evans, T. M. (2019). Discrete numerical simulations of torpedo anchor installation in granular soils. Computers and Geotechnics, 108, 40-52.